ACS Partner Journal

PHOTON SCIENCE

pubs.acs.org/photonsci

Article

The Disulfide Bond in S $L_{2,3}$ X-ray Emission Spectroscopy of Transition Metal Sulfides

Lothar Weinhardt,* Dirk Hauschild, Constantin Wansorra, Ralph Steininger, Jörg Göttlicher, Monika Blum, Wanli Yang, and Clemens Heske

Cite This: https://doi.org/10.1021/photonsci.6c00007

Read Online

ACCESS | Metrics & More | Article Recommendations | Supporting Information

ABSTRACT: S $L_{2,3}$ X-ray emission spectroscopy (XES) and spectra calculations based on density functional theory are used to study the electronic valence structure of Mn, Fe, Co, and Cu transition metal sulfides, without (MnS, FeS, CoS, and Cu_2S) and with (MnS_2, FeS_2, CoS_2, and CuS) sulfur dimers in the crystal structure. We find the upper valence band region in the experimental spectra to be very sensitive to the transition metal, while a splitting in the transitions from the S 3s derived bands indicates the presence of sulfur dimers. This makes S $L_{2,3}$ XES particularly well suited to the chemical speciation of these compounds. The spectral changes are reproduced by our spectra calculations, which allows for a detailed understanding of the electronic structure based on the band structure and the projected density of states. The splitting of the S 3s derived bands in the dimer compounds is found to increase with decreasing sulfur−sulfur distance, indicating an increase of covalency. The splitting in our experimental XES spectra is found to be smaller than in photoemission data and our spectra calculations, which we attribute to nuclear dynamics on the time scale of the X-ray emission process. In particular, the high sensitivity of S $L_{2,3}$ XES to the presence of sulfur dimers, together with its suitability for operando studies, makes it a key technique for future studies on a wide range of relevant material systems.

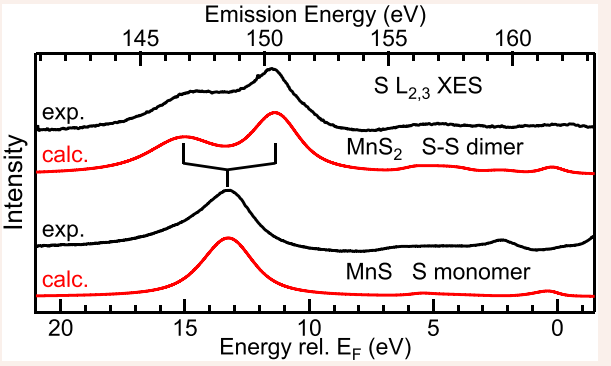

KEYWORDS: *X-ray emission spectroscopy (XES), transition metal sulfides, valence bond, sulfur dimers*

INTRODUCTION

Transition metal sulfides play an important role in many applications. These include the use of NiS_2 as a low-cost electrode material for high-performance supercapacitors,[1] NiS_2, NiS, and Ni_3S_4 electrocatalysts for hydrogen production in seawater,[2] or FeS_2-based materials for batteries.[3] Further examples are CoS_2, Co_9S_8, CoS, FeS_2, and MoS_2 as anodes in Li-ion batteries[4] and M_xS_y (M = Fe, Co, Ni, etc.) as bifunctional electrocatalysts for water splitting.[5] In particular, earth-abundant metal pyrites (FeS_2, CoS_2, NiS_2, and their alloys) are highly efficient for electrocatalytic hydrogen evolution and polysulfide reduction.[6] It is suggested that, in these materials, the transition metal as well as the disulfide anions (S_2^{2-}) play an active role in high catalytic activity.[6]

Due to their importance, the geometric, electronic, and chemical structures of transition metal sulfides have been characterized extensively. For chemical speciation and electronic structure evaluation, electron and X-ray spectroscopy techniques have been employed. Much of that work has focused on the metal states, including 2p X-ray photoelectron spectroscopy (XPS)[7−12] and K and $L_{2,3}$ edge X-ray absorption spectroscopy (XAS).[12−16] But also S 2p XPS,[7−9,12] S K,[13,15,17−19] and $L_{2,3}$[14,20,21] XAS have been employed, giving detailed insights into these compounds.

X-ray emission spectroscopy (XES) has also been used to study transition metal sulfides, both for metal[15,22−25] and sulfur[15,17,26−28] K and $L_{2,3}$ edges. The local character of XES, probing the chemical environment around a selected core level, makes it very powerful for chemical speciation, particularly in mixed compounds with many constituents. This, together with its suitability for operando studies, makes XES a very powerful technique for applied materials studies. To probe the local environment around the sulfur atoms, most commonly S K XES has been employed. In this study, we focus on S $L_{2,3}$ XES, with a particular emphasis on the S 3s derived valence bands, which are not visible in S K XES due to the dipole selection rules.

The S $L_{2,3}$ XES spectra are very sensitive to the chemical environment of sulfur, probing valence states of s and d symmetry, which was already recognized in an early pioneering study by O'Bryan and Skinner.[28] Besides their sensitivity to the

Received: February 2, 2026
Revised: March 6, 2026
Accepted: March 6, 2026

S oxidation state,[27] sulfur compounds with the same oxidation state, which would not show a discernible core level shift in XPS, like sulfides[27,29,30] or sulfates,[31] can be easily distinguished. Of the transition metal sulfides addressed in the present study, S $L_{2,3}$ spectra for MnS,[28] Cu_2S,[14,19,20,27,28,32,33] CuS,[14,19,27,34] and FeS_2[34] are found in the literature.

In this study, we investigate a systematic series of transition metal sulfides *without* (MnS, FeS, CoS, and Cu_2S) and with (MnS_2, FeS_2, CoS_2, and CuS) sulfur dimers in the crystal structure to derive and understand the signature of the disulfide bond in S $L_{2,3}$ XES.

EXPERIMENTAL SECTION

Experiments were performed in two different experimental setups. The spectra for MnS, FeS, FeS_2, Cu_2S, and CuS were measured using the high-transmission spectrometer[35] of the Solid and Liquid Spectroscopic Analysis (SALSA) roll-up experimental station[36] at Beamline 8.0.1 of the Advanced Light Source (ALS), Lawrence Berkeley National Laboratory (Berkeley, USA). The energy scale for the SALSA data was calibrated as described in ref 29, giving an absolute (relative) uncertainty of 0.1 eV (0.03 eV). The MnS_2, CoS, and CoS_2 data were measured with the high-transmission spectrometer[37] of the X-SPEC beamline[38] at the KIT Light Source. The energy scale for these measurements was calibrated using a $CaSO_4$ reference measurement for an absolute uncertainty of 0.1 eV. For both instruments, the experiments were run with a combined energy resolution (beamline and spectrometer) of 0.25 eV, as determined from the full-width at half-maximum of the elastic scattered peaks.

For the experiments at the ALS, MnS, FeS, FeS_2, Cu_2S, and CuS powders were purchased and shipped under argon from Alfa Aesar. The powders were fixed to the sample holder by pressing them onto double-sided and ultrahigh vacuum-compatible tape in a nitrogen-filled glove box. The samples were then transported in a nitrogen-filled container to the experimental station and loaded into vacuum without air exposure using a nitrogen-filled glove bag. For the experiments at the KIT Light Source, CoS and CoS_2 powders were purchased and shipped under argon from Fisher Scientific and pressed into thin pellets in an argon-filled glove box. For MnS_2, a hauerite crystal from the Jeziórko mine in Tarnobrzeg (Poland) was cleaved in an argon-filled glove box. The samples were then transported to the beamline in an argon-filled sample container, which was then directly attached to the experimental station and transferred without any air exposure.

THEORY

To calculate band structures, projected densities of states (PDOS), and XES spectra, we have used Wien2k, which uses the full-potential augmented plane wave plus local orbitals (APW+lo) method to solve the Kohn–Sham density functional theory (DFT) equations.[39] Exchange–correlation effects were described by the generalized gradient approximation (GGA) as parameterized by Perdew, Burke, and Ernzerhof (PBE).[40] XES spectra were calculated from the PDOS using the dipole approximation and Fermi's Golden Rule in the formalism described by Schwarz et al.[41−43] 1000 *k* points were used for the self-consistent field (SCF) cycle, except for Cu_2S with 100 *k* points. For the PDOS and XES spectra calculations, 10,000 *k* points were used (1000 *k* points for Cu_2S). The crystal structures (see Figures S1−S8 in the Supporting Information) were obtained from the Materials Project Database[44] with the materials IDs mp-504 (CuS), mp-2070 (CoS_2), mp-226 (FeS_2), mp-581212 (Cu_2S), mp-1274 (CoS), mp-2099 (FeS), and mp-2065 (MnS) and the Crystallography Open Database, ID 1011237 (MnS_2).[45]

In addition to the calculations of the transition metal sulfide crystals, we have used the StoBe-DeMon 3.3 DFT code[46] to calculate the orbital energies of an isolated S_2^{2-} ion as a function of sulfur–sulfur distance. The calculations used the Becke–Perdew gradient-corrected exchange and correlation functionals,[47−49] triple ζ bases[50] to describe the valence electrons, and effective core potentials (ECPs)[51] with 73111/6111/1 basis sets. The auxiliary basis sets were composed of five s and four spd functions for sulfur to fit the Coulomb and exchange–correlation potentials.

RESULTS AND DISCUSSION

Figure 1 shows the experimental XES spectra of the investigated samples, excited with photon energies well above

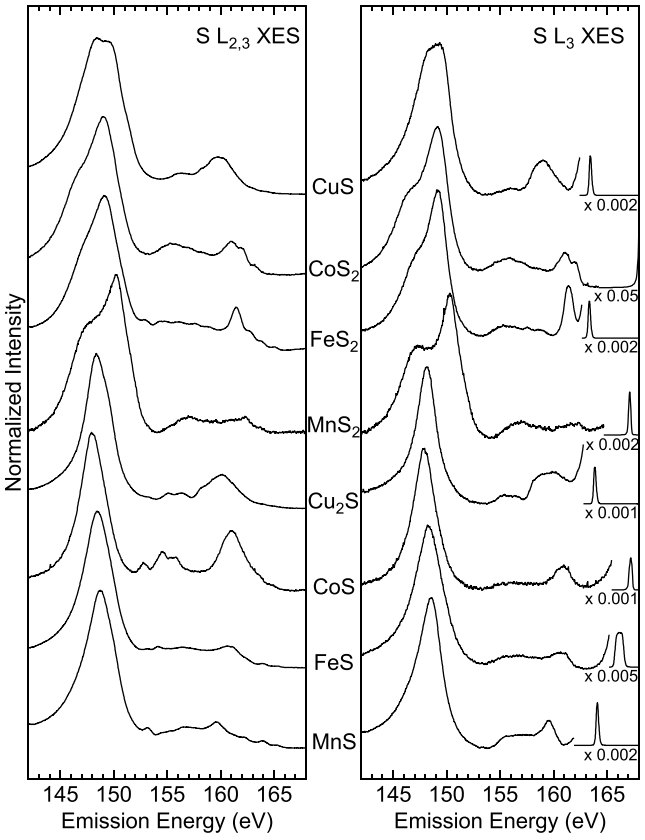

Figure 1. Experimental S $L_{2,3}$ (left) and S L_3 (right) XES spectra of (from top to bottom) CuS, CoS_2, FeS_2, MnS_2, Cu_2S, CoS, FeS, and MnS. For S $L_{2,3}$, excitation energies of 184.6 eV (CuS, FeS_2, Cu_2S, FeS, and MnS) and 200.3 eV (CoS_2, MnS_2, and CoS) were used. The S L_3 spectra were excited just below the S L_2 onset, i.e., with 163.4 eV (CuS and FeS_2), 168.2 eV (CoS_2), 167.1 eV (MnS_2), 163.9 eV (Cu_2S), 167.2 eV (CoS), 166.2 eV (FeS), and 164.1 eV (MnS).

the absorption onset (S $L_{2,3}$, left) and in-between the L_3 and L_2 edges (L_3, right). The spectra contain transitions from valence states that exhibit wave function overlap with the S 2p core levels and obey the dipole selection rule $\Delta l = \pm 1$, i.e., probing valence states of s and d symmetry. The valence bands of the

https://doi.org/10.1021/photonsci.6c00007
Photon Sci. XXXX, XXX, XXX−XXX

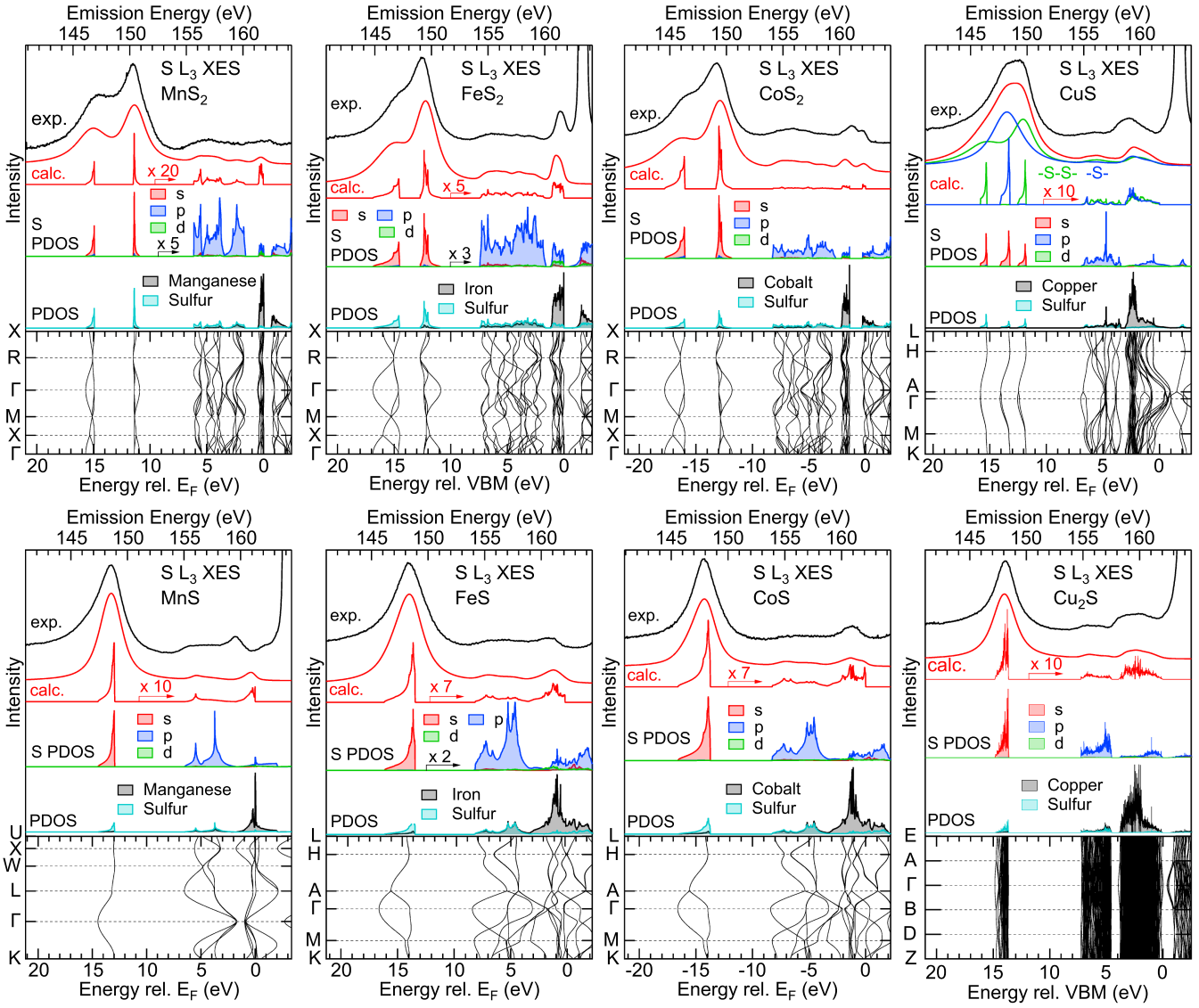

Figure 2. Comparison of the experimental S L_3 XES spectra of the investigated compounds ("exp.", top spectrum in each panel) with calculations based on DFT ("calc."). The bottom and top rows show compounds with S monomers and dimers in the crystal structure, respectively. Each panel shows (from bottom to top): calculated band structure, density of states projected onto atomic species (PDOS), symmetries for the sulfur atoms (S PDOS), calculated S L_3 XES spectrum without and with experimental and lifetime broadening (both red), and the experimental spectrum (black). The theory energy scales on the bottom and the experimental emission energy scales on the top were shifted to align the most prominent spectral features in theory and experiment. In some cases, the ordinates of the S PDOS and the unbroadened S L_3 calculations were multiplied by the factors given (upper valence band region only).

transition metal sulfides investigated are derived from the S 3s and 3p as well as the metal 3d and 4s states. Due to suitable symmetry and large overlap with the S 2p states, all spectra are dominated by transitions from S 3s derived bands around 148.5 eV. The upper valence bands are dominated by S 3p derived bands around the sulfur atoms, and we thus only find weak emission above 154 eV from sulfur s and d admixtures to these bands. As can be seen in Figure 1, this latter spectral region is very sensitive to the specific metal bonding partner and can serve as a "fingerprint" tool. While compounds with the same metal exhibit similarities in this region, we still find distinct differences that allow for a speciation of the respective compound.

Different from the upper valence band region, the peak assigned to transitions from S 3s derived bands at ~148.5 eV ("S 3s" in the following) shows much less dependence on the metal of the compound. In fact, only small changes in line widths are observed for this feature between the spectra of Cu_2S, CoS, FeS, and MnS due to differences in lifetime broadening. In contrast, a splitting of the "S 3s" peak is observed for CuS (also observed in refs 19,27,34), CoS_2, FeS_2 (also in ref 34), and MnS_2. This is a consequence of the splitting of the S 3s derived bands by the covalent disulfide bond in these compounds and will be discussed in more detail below.

We note that the S $L_{2,3}$ spectra mainly differ from the L_3 spectra by containing all features twice, with an L_3/L_2 intensity ratio of 2:1 and separated by the spin−orbit splitting of the S 2p core levels (1.20 eV[52,53]). The one exception is found for our CoS data; this sample was partially oxidized, leading to sulfate and sulfite contributing to the S $L_{2,3}$ XES spectrum at 152.8, 154.5, 155.7, and ~161 eV. In contrast, the L_3 spectra

https://doi.org/10.1021/photonsci.6c00007
Photon Sci. XXXX, XXX, XXX−XXX

are free of these artifacts since they are excited below the absorption edge of sulfates and sulfites. In the following, we will thus discuss the "simpler" L_3 spectra in more detail to avoid any sulfate, sulfite, and L_2 contributions.

For this discussion, Figure 2 compares the experimental S L_3 spectra with calculations based on DFT. For each compound, Figure 2 shows (from bottom to top) the calculated band structure, density of states projected onto atomic species (PDOS) and symmetries for the sulfur atoms (S PDOS), the calculated S L_3 XES spectrum without and with experimental and lifetime broadening (both red), and the experimental spectrum (black). Overall, the calculations give a very good description of the experimental spectra, and we observe the following trends: the upper valence bands are mainly comprised of states of p symmetry, located near the sulfur atoms (at higher binding energies), and of d symmetry, located near the metal atoms (at lower binding energies). Neither the states of pure p symmetry located at the sulfur atoms (being dipole-forbidden) nor the states of d symmetry localized at the metal atoms (due to missing wave function overlap with the S 2p core levels) give rise to spectral intensity in the S L_3 XES spectra. However, we find some degree of hybridization between S 3s and S 3p, leading to s symmetric S PDOS in the region of the sulfur p bands. Also, hybridization between S 3d and the metal d states is observed, leading to d symmetric S PDOS in the region of the metal d bands. These states are reflected in the S L_3 XES spectra as a broader structure between emission energies of approx. 154 to 158 eV and emission at or slightly above 158 eV, respectively. As a general trend, the increasing occupation of the metal d states with increasing atomic number is reflected in an increase of the occupied metal PDOS below the VBM (or E_F) as well as an increase of hybridization with the S 3d states. This is most prominently visible for the copper sulfides, where the intensity increases above 158 eV.

As expected, we find predominantly s symmetric S PDOS in the region of the "S 3s" peak(s). For the compounds with exclusively S monomers, we observe one band (MnS) or one group of bands (FeS, CoS, and Cu_2S), while the compounds with S dimers exhibit two (MnS_2, FeS_2, and CoS_2) clearly split groups of bands. For CuS, three groups of S 3s derived bands are found, two of which are due to sulfur dimers and the third due to sulfur monomers within the compound. In a simple molecular orbital picture, the splitting of the bands in the sulfur dimers is caused by hybridization of the S 3s orbitals, forming bonding and antibonding "molecular" orbitals (at higher and lower binding energies, respectively).

We find the magnitude of this splitting to vary among the different compounds, which is investigated in conjunction with Figure 3. There, values for the S 3s splitting are derived from our experimental XES spectra (black circles), from the corresponding DFT spectra calculations (green squares), from experimental photoemission spectra taken from literature[10,54] (blue diamonds), as well as from DFT calculations of an isolated S_2^{2-} ion (red line). Overall and as expected, the S 3s splitting decreases as a function of increasing S−S distance. The calculated values for the S_2^{2-} ion lie significantly above the values of the solids, which we attribute to the missing environment in the case of the isolated ion.

The splitting values calculated for the different solid compounds (i.e., those investigated here, plus NiS_2) are in good agreement with the literature values[10,54] from photoemission experiments. In contrast, we find our XES experiments to yield a significantly smaller splitting than in both calculations and photoemission experiments. While the former could potentially indicate shortcomings in the energy scale of the calculation (as is not unusual for DFT approaches), photoemission and XES nominally share the same final state and are thus expected to give the same energy difference based on the final-state rule.[55] We attribute the decreased splitting to the finite duration of the XES process, during which ultrafast nuclear dynamics occur. The time scale is governed by the core-hole lifetime (~16 fs for S 2p[56]), and thus symmetry breaking,[57] vibrational excitation,[58−60] as well as full dissociation of molecules[61−65] (among others) can occur on that time scale.

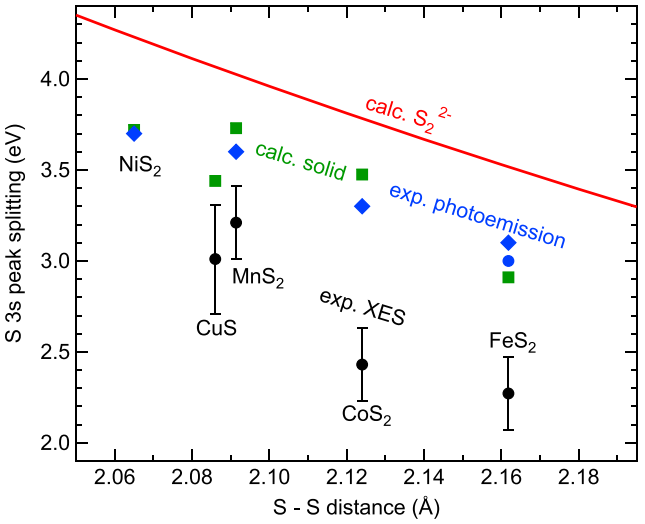

Figure 3. S 3s peak splitting for the studied compounds as a function of S−S distance (taken from the same crystal structures used in the calculations), determined experimentally by XES (black circles, this work) and photoelectron spectroscopy[10,54] (blue diamonds), as well as calculated based on DFT (green squares). For comparison, the splitting calculated for an isolated S_2^{2-} ion of varied S−S distance is shown as a red line.

To understand these dynamics for the sulfur dimer, Figure 4 shows the potential energy curves of the S_2^{2-} ion in the ground (black), lowest core-excited (red), and core-ionized (green) states, as derived from our DFT calculations. The exciting X-ray will create a wave packet located at the equilibrium bond distance of the ground state, which will move along the potential energy surface of the excited state until emission takes place. In general, this will increase the S−S distance in the final state and thus lead to a smaller splitting (and to a peak broadening) in the XES spectra. If we take the slope of the red curve in Figure 3, we see a decrease in splitting of ~0.5 eV, as roughly observed between exp. XES and PES/calc. solid, which would correspond to a S−S distance increase of ~0.07 Å. This is a rather small change in distance, similar to the S−S distance difference between CuS and FeS_2.

CONCLUSIONS

The electronic valence band structure of a series of Mn, Fe, Co, and Cu transition metal sulfides has been investigated using S $L_{2,3}$ soft X-ray emission spectroscopy (XES). We have studied compounds with sulfur dimers (CuS, CoS_2, MnS_2, and FeS_2) and without sulfur dimers (Cu_2S, CoS, FeS, and MnS) in the structure. The XES spectra provide unique fingerprints for each compound that can be understood and used for chemical

https://doi.org/10.1021/photonsci.6c00007
Photon Sci. XXXX, XXX, XXX−XXX

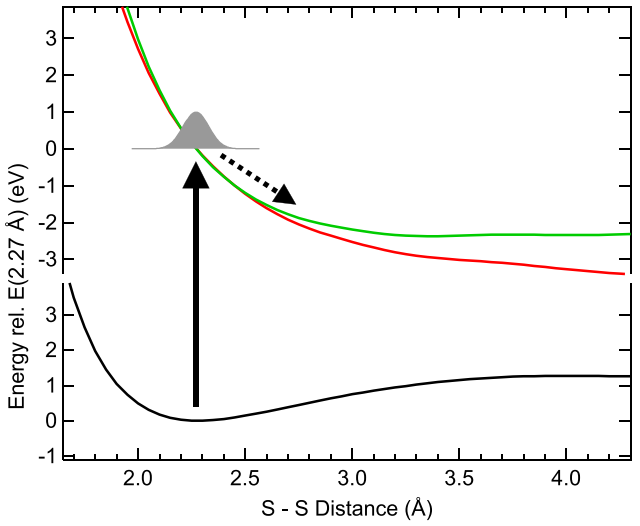

Figure 4. Calculated potential energy curves of the S_2^{2-} ion in the ground (black), lowest core-excited (red), and core-ionized (green) states. The vertical arrow indicates the X-ray excitation that creates a wave packet in the excited state (gray Gaussian), which will move along the potential energy curve (dashed arrow).

speciation. We find that the upper valence band region in the spectra is very sensitive to the metal bonding partner of sulfur in the compounds, which can be understood in detail using spectra calculations based on DFT. Furthermore, we find a splitting of the S 3s band in the compounds containing *S* dimers, which decreases with increasing S−S distance. While this qualitative change agrees with our spectra calculations as well as with photoemission experiments in the literature, we find the splitting in XES to be less than the photoemission values and those predicted by our ground state calculations. This is assigned to ultrafast dynamics on the femtosecond time scale of the X-ray emission process that leads to a S−S bond elongation upon X-ray excitation. The demonstrated high sensitivity of S $L_{2,3}$ XES to the S−S dimer bond is expected to give crucial insights for a wide range of applied material systems.

■ ASSOCIATED CONTENT

Supporting Information

The Supporting Information is available free of charge at https://pubs.acs.org/doi/10.1021/photonsci.6c00007.

Crystal structures of the investigated compounds (PDF)

■ AUTHOR INFORMATION

Corresponding Author

Lothar Weinhardt − *Institute for Photon Science and Synchrotron Radiation (IPS) and Institute for Chemical Technology and Polymer Chemistry (ITCP), Karlsruhe Institute of Technology (KIT), 76131 Karlsruhe, Germany; Department of Chemistry and Biochemistry, University of Nevada, Las Vegas (UNLV), Las Vegas, Nevada 89154, United States;* orcid.org/0000-0003-3361-1054; Email: Lothar.Weinhardt@kit.edu

Authors

Dirk Hauschild − *Institute for Photon Science and Synchrotron Radiation (IPS) and Institute for Chemical Technology and Polymer Chemistry (ITCP), Karlsruhe Institute of Technology (KIT), 76131 Karlsruhe, Germany; Department of Chemistry and Biochemistry, University of Nevada, Las Vegas (UNLV), Las Vegas, Nevada 89154, United States;* orcid.org/0000-0001-9088-8944

Constantin Wansorra − *Institute for Photon Science and Synchrotron Radiation (IPS), Karlsruhe Institute of Technology (KIT), 76131 Karlsruhe, Germany; Department of Chemistry and Biochemistry, University of Nevada, Las Vegas (UNLV), Las Vegas, Nevada 89154, United States;* orcid.org/0000-0002-7120-8322

Ralph Steininger − *Institute for Photon Science and Synchrotron Radiation (IPS), Karlsruhe Institute of Technology (KIT), 76131 Karlsruhe, Germany*

Jörg Göttlicher − *Institute for Photon Science and Synchrotron Radiation (IPS), Karlsruhe Institute of Technology (KIT), 76131 Karlsruhe, Germany*

Monika Blum − *Department of Chemistry and Biochemistry, University of Nevada, Las Vegas (UNLV), Las Vegas, Nevada 89154, United States; Advanced Light Source (ALS), Lawrence Berkeley National Laboratory, Berkeley, California 94720, United States; Chemical Sciences Division, Lawrence Berkeley National Laboratory, Berkeley, California 94720, United States;* orcid.org/0000-0002-2918-9092

Wanli Yang − *Advanced Light Source (ALS), Lawrence Berkeley National Laboratory, Berkeley, California 94720, United States;* orcid.org/0000-0003-0666-8063

Clemens Heske − *Institute for Photon Science and Synchrotron Radiation (IPS) and Institute for Chemical Technology and Polymer Chemistry (ITCP), Karlsruhe Institute of Technology (KIT), 76131 Karlsruhe, Germany; Department of Chemistry and Biochemistry, University of Nevada, Las Vegas (UNLV), Las Vegas, Nevada 89154, United States;* orcid.org/0000-0001-7586-4549

Complete contact information is available at: https://pubs.acs.org/10.1021/photonsci.6c00007

Notes

The authors declare no competing financial interest.

■ ACKNOWLEDGMENTS

This research used resources of the Advanced Light Source, which is a DOE Office of Science User Facility under contract no. DE-AC02-05CH11231. We gratefully acknowledge the outstanding support by the ALS safety team, in particular Doug Taube and Alyssa Brand. D. Hauschild, L. Weinhardt, and C. Heske thank the Deutsche Forschungsgemeinschaft (DFG) for funding in projects GZ:INST 121384/65-1 FUGG and GZ:INST 121384/66-1 FUGG.

■ REFERENCES

(1) Thomas, S. A.; Cherusseri, J.; Rajendran, D. N. Nickel Disulfide (NiS_2): A Sustainable Low-Cost Electrode Material for High-Performance Supercapacitors. *Energy Technol.* **2024**, *12* (7), No. 2400138.

(2) Li, M.; Li, H.; Fan, H.; Liu, Q.; Yan, Z.; Wang, A.; Yang, B.; Wang, E. Engineering Interfacial Sulfur Migration in Transition-Metal Sulfide Enables Low Overpotential for Durable Hydrogen Evolution in Seawater. *Nat. Commun.* **2024**, *15* (1), No. 6154.

(3) Whang, G.; Zeier, W. G. Transition Metal Sulfide Conversion: A Promising Approach to Solid-State Batteries. *ACS Energy Lett.* **2023**, *8* (12), 5264−5274.

(4) Wang, S.; Qu, C.; Wen, J.; Wang, C.; Ma, X.; Yang, Y.; Huang, G.; Sun, H.; Xu, S. Progress of Transition Metal Sulfides Used as

Lithium-Ion Battery Anodes. *Mater. Chem. Front.* **2023**, *7* (14), 2779−2808.
(5) Wang, M.; Zhang, L.; He, Y.; Zhu, H. Recent Advances in Transition-Metal-Sulfide-Based Bifunctional Electrocatalysts for Overall Water Splitting. *J. Mater. Chem. A* **2021**, *9* (9), 5320−5363.
(6) Faber, M. S.; Lukowski, M. A.; Ding, Q.; Kaiser, N. S.; Jin, S. Earth-Abundant Metal Pyrites (FeS_2, CoS_2, NiS_2, and Their Alloys) for Highly Efficient Hydrogen Evolution and Polysulfide Reduction Electrocatalysis. *J. Phys. Chem. C* **2014**, *118* (37), 21347−21356.
(7) Laajalehto, K.; Kartio, I.; Nowak, P. XPS Study of Clean Metal Sulfide Surfaces. *Appl. Surf. Sci.* **1994**, *81* (1), 11−15.
(8) Karthe, S.; Szargan, R.; Suoninen, E. Oxidation of Pyrite Surfaces: A Photoelectron Spectroscopic Study. *Appl. Surf. Sci.* **1993**, *72* (2), 157−170.
(9) Perry, D. L.; Taylor, J. A. X-ray Photoelectron and Auger Spectroscopic Studies of Cu_2S and CuS. *J. Mater. Sci. Lett.* **1986**, *5* (4), 384−386.
(10) van der Heide, H.; Hemmel, R.; van Bruggen, C. F.; Haas, C. X-ray Photoelectron Spectra of 3d Transition Metal Pyrites. *J. Solid State Chem.* **1980**, *33* (1), 17−25.
(11) Folmer, J. C. W.; Jellinek, F. The Valence of Copper in Sulphides and Selenides: An X-ray Photoelectron Spectroscopy Study. *J.Less-Common Met.* **1980**, *76* (1), 153−162.
(12) Goh, S. W.; Buckley, A. N.; Lamb, R. N. Copper(II) Sulfide? *Miner. Eng.* **2006**, *19* (2), 204−208.
(13) Womes, M.; Karnatak, R. C.; Esteva, J. M.; Lefebvre, I.; Allan, G.; Olivier-fourcades, J.; Jumas, J. C. Electronic Structures of FeS and FeS_2: X-ray Absorption Spectroscopy and Band Structure Calculations. *J. Phys. Chem. Solids* **1997**, *58* (2), 345−352.
(14) Vegelius, J. R.; Kvashnina, K. O.; Hollmark, H.; Klintenberg, M.; Kvashnin, Y. O.; Soroka, I. L.; Werme, L.; Butorin, S. M. X-ray Spectroscopic Study of Cu_2S, CuS, and Copper Films Exposed to Na_2S Solutions. *J. Phys. Chem. C* **2012**, *116* (42), 22293−22300.
(15) Kumar, P.; Nagarajan, R.; Sarangi, R. Quantitative X-ray Absorption and Emission Spectroscopies: Electronic Structure Elucidation of Cu_2S and CuS. *J. Mater. Chem. C* **2013**, *1* (13), 2448−2454.
(16) Sugiura, C. Iron K X-ray Absorption-edge Structures of FeS and FeS_2. *J. Chem. Phys.* **1984**, *80* (3), 1047−1049.
(17) Sugiura, C.; Gohshi, Y.; Suzuki, I. Sulfur K $_\beta$ X-ray Emission Spectra and Electronic Structures of Some Metal Sulfides. *Phys. Rev. B* **1974**, *10* (2), No. 338.
(18) Kravtsova, A. N.; Stekhin, I. E.; Soldatov, A. V.; Liu, X.; Fleet, M. E. Electronic Structure of MS (M=Ca,Mg,Fe,Mn): X-ray Absorption Analysis. *Phys. Rev. B* **2004**, *69* (13), No. 134109.
(19) Sugiura, C.; Yamasaki, H.; Shoji, T. X-ray Spectra and Electronic Structures of CuS and Cu_2S. *J. Phys. Soc. Jpn.* **1994**, *63* (3), 1172−1178.
(20) Bär, M.; Schubert, B.-A.; Marsen, B.; Schorr, S.; Wilks, R. G.; Weinhardt, L.; Pookpanratana, S.; Blum, M.; Krause, S.; Zhang, Y.; Yang, W.; Unold, T.; Heske, C.; Schock, H.-W. Electronic Structure of Cu_2ZnSnS_4 Probed by Soft X-ray Emission and Absorption Spectroscopy. *Phys. Rev. B* **2011**, *84* (3), No. 035308.
(21) Kravtsova, A. N.; Stekhin, I. E.; Soldatov, A. V.; Fleet, M. E.; Harmer, S. L. Local and Electronic Structure of FeS, CoS, NiS: Ultrasoft Sulfur L2,3 X-ray Absorption Spectra Analysis. *J. Electron Spectrosc. Relat. Phenom.* **2005**, *144−147*, 525−527.
(22) Joe, Y. I.; O'Neil, G. C.; Miaja-Avila, L.; Fowler, J. W.; Jimenez, R.; Silverman, K. L.; Swetz, D. S.; Ullom, J. N. Observation of Iron Spin-States Using Tabletop X-ray Emission Spectroscopy and Microcalorimeter Sensors. *J. Phys. B:At., Mol. Opt. Phys.* **2016**, *49* (2), No. 024003.
(23) Sato, K.; Harada, Y.; Taguchi, M.; Shin, S.; Fujimori, A. Characterization of Fe 3d States in $CuFeS_2$ by Resonant X-ray Emission Spectroscopy. *Phys. Status Solidi A* **2009**, *206* (5), 1096−1100.
(24) Wansleben, M.; Vinson, J.; Wählisch, A.; Bzheumikhova, K.; Hönicke, P.; Beckhoff, B.; Kayser, Y. Speciation of Iron Sulfide Compounds by Means of X-ray Emission Spectroscopy Using a Compact Full-Cylinder von Hamos Spectrometer. *J. Anal. At. Spectrom.* **2020**, *35* (11), 2679−2685.
(25) Mortensen, D. R.; Seidler, G. T.; Kas, J. J.; Govind, N.; Schwartz, C. P.; Pemmaraju, S.; Prendergast, D. G. Benchmark Results and Theoretical Treatments for Valence-to-Core X-ray Emission Spectroscopy in Transition Metal Compounds. *Phys. Rev. B* **2017**, *96* (12), No. 125136.
(26) Mori, R. A.; Paris, E.; Giuli, G.; Eeckhout, S. G.; Kavčič, M.; Žitnik, M.; Bučar, K.; Pettersson, L. G. M.; Glatzel, P. Electronic Structure of Sulfur Studied by X-ray Absorption and Emission Spectroscopy. *Anal. Chem.* **2009**, *81* (15), 6516−6525.
(27) Heske, C.; Groh, U.; Fuchs, O.; Umbach, E.; Franco, N.; Bostedt, C.; Terminello, L. J.; Perera, R. C. C.; Hallmeier, K. H.; Preobrajenski, A.; Szargan, R.; Zweigart, S.; Riedl, W.; Karg, F. X-ray Emission Spectroscopy of $Cu(In,Ga)(S,Se)_2$-Based Thin Film Solar Cells: Electronic Structure, Surface Oxidation, and Buried Interfaces. *Phys. Status Solidi A* **2001**, *187* (1), 13−24.
(28) O'Bryan, H. M.; Skinner, H. W. B. The Soft X-ray Spectroscopy of Solids. II. Emission Spectra from Simple Chemical Compounds. *Proc. R. Soc. London, Ser. A* **1940**, *176* (965), 229−262.
(29) Weinhardt, L.; Hauschild, D.; Fuchs, O.; Steininger, R.; Jiang, N.; Blum, M.; Denlinger, J. D.; Yang, W.; Umbach, E.; Heske, C. Satellite-Dominated Sulfur $L_{2,3}$ X-ray Emission of Alkaline Earth Metal Sulfides. *ACS Omega* **2023**, *8*, 4921−4927.
(30) Weinhardt, L.; Hauschild, D.; Wansorra, C.; Steininger, R.; Blum, M.; Yang, W.; Heske, C. Valence-Band Hybridization in Sulphides. *Phys. Chem. Chem. Phys.* **2024**, *26* (41), 26389−26397.
(31) Weinhardt, L.; Hauschild, D.; Steininger, R.; Jiang, N.; Blum, M.; Yang, W.; Heske, C. Sulfate Speciation Analysis Using Soft X-ray Emission Spectroscopy. *Anal. Chem.* **2021**, *93* (23), 8300−8308.
(32) Zhang, L.; Wett, D.; Schulze, D.; Szargan, R.; Nagel, M.; Peisert, H.; Chassé, T. Chemical Reactions at Cu/ZnS(001) and In/ZnS(001) Heterojunctions: A Comparison of Photoelectron and S $L_{2,3}$ X-ray Emission Spectroscopy. *Appl. Phys. Lett.* **2005**, *86* (1), No. 012108.
(33) Hauschild, D.; Wachs, S. J.; Kogler, W.; Seitz, L.; Carter, J.; Schnabel, T.; Krause, B.; Blum, M.; Yang, W.; Ahlswede, E.; Heske, C.; Weinhardt, L. Chemical Structure of a Carbon-Rich Layer at the Wet-Chemical Processed $Cu_2ZnSn(S,Se)_4$/Mo Interface. *IEEE J. Photovoltaics* **2021**, *11* (3), No. 658.
(34) Kurmaev, E. Z.; van Ek, J.; Ederer, D. L.; Zhou, L.; Callcott, T. A.; Perera, R. C. C.; Cherkashenko, V. M.; Shamin, S. N.; Trofimova, V. A.; Bartkowski, S.; Neumann, M.; Fujimori, A.; Moloshag, V. P. Experimental and Theoretical Investigation of the Electronic Structure of Transition Metal Sulphides: CuS, And. *J. Phys. Condens. Matter* **1998**, *10* (7), No. 1687.
(35) Fuchs, O.; Weinhardt, L.; Blum, M.; Weigand, M.; Umbach, E.; Bär, M.; Heske, C.; Denlinger, J.; Chuang, Y. D.; McKinney, W.; Hussain, Z.; Gullikson, E.; Jones, M.; Batson, P.; Nelles, B.; Follath, R. High-Resolution, High-Transmission Soft X-ray Spectrometer for the Study of Biological Samples. *Rev. Sci. Instrum.* **2009**, *80* (6), No. 63103.
(36) Blum, M.; Weinhardt, L.; Fuchs, O.; Bär, M.; Zhang, Y.; Weigand, M.; Krause, S.; Pookpanratana, S.; Hofmann, T.; Yang, W.; Denlinger, J. D.; Umbach, E.; Heske, C. Solid and Liquid Spectroscopic Analysis (SALSA) - a Soft X-ray Spectroscopy Endstation with a Novel Flow-through Liquid Cell. *Rev. Sci. Instrum.* **2009**, *80* (12), No. 123102.
(37) Weinhardt, L.; Wansorra, C.; Steininger, R.; Spangenberg, T.; Hauschild, D.; Heske, C. High-Transmission Spectrometer for Rapid Resonant Inelastic Soft X-ray Scattering (rRIXS) Maps. *J. Synchrotron Radiat.* **2024**, *31* (6), 1481−1488.
(38) Weinhardt, L.; Steininger, R.; Kreikemeyer-Lorenzo, D.; Mangold, S.; Hauschild, D.; Batchelor, D.; Spangenberg, T.; Heske, C. X-SPEC: A 70 eV to 15 keV Undulator Beamline for X-ray and Electron Spectroscopies. *J. Synchrotron Radiat.* **2021**, *28* (2), 609−617.

https://doi.org/10.1021/photonsci.6c00007
Photon Sci. XXXX, XXX, XXX−XXX

(39) Blaha, P.; Schwarz, K.; Tran, F.; Laskowski, R.; Madsen, G. K. H.; Marks, L. D. WIEN2k: An APW+lo Program for Calculating the Properties of Solids. *J. Chem. Phys.* **2020**, *152* (7), No. 074101.
(40) Perdew, J. P.; Burke, K.; Ernzerhof, M. Generalized Gradient Approximation Made Simple. *Phys. Rev. Lett.* **1996**, *77* (18), No. 3865.
(41) Neckel, A.; Schwarz, K.; Eibler, R.; Rastl, P.; Weinberger, P. Elektronische Struktur und Valenzbandspektren einiger metallischer Hartstoffe. In *Mikrochimica Acta*; Zacherl, M. K., Ed.; Springer: Vienna, 1975; pp 257−291 DOI: 10.1007/978-3-7091-8422-6_20.
(42) Schwarz, K.; Neckel, A.; Nordgren, J. On the X-ray Emission Spectra from FeAl. *J. Phys. F: Met. Phys.* **1979**, *9* (12), 2509−2521.
(43) Schwarz, K.; Wimmer, E. Electronic Structure and X-ray Emission Spectra of YS in Comparison with NbC. *J. Phys. F: Met. Phys.* **1980**, *10* (5), 1001−1012.
(44) Jain, A.; Ong, S. P.; Hautier, G.; Chen, W.; Richards, W. D.; Dacek, S.; Cholia, S.; Gunter, D.; Skinner, D.; Ceder, G.; Persson, K. A. Commentary: The Materials Project: A Materials Genome Approach to Accelerating Materials Innovation. *APL Mater.* **2013**, *1* (1), No. 011002.
(45) Offner, F. A Redetermination of the Parameter for Hauerite, MnS_2. *Z. Kristallogr. - Cryst. Mater.* **1934**, *89* (1−6), 182−184.
(46) Hermann, K.; Pettersson, L. G. M.; Casida, M. E.; Daul, C.; Goursot, A.; Koester, A.; Proynov, E.; St-Amant, A.; Salahub, D. R.et al. StoBe-deMon Version 3.3. 2014.
(47) Becke, A. D. Density-Functional Exchange-Energy Approximation with Correct Asymptotic Behavior. *Phys. Rev. A* **1988**, *38* (6), No. 3098.
(48) Perdew, J. P. Density-Functional Approximation for the Correlation Energy of the Inhomogeneous Electron Gas. *Phys. Rev. B* **1986**, *33* (12), No. 8822.
(49) Perdew, J. P. Erratum: Density-Functional Approximation for the Correlation Energy of the Inhomogeneous Electron Gas. *Phys. Rev. B* **1986**, *34* (10), No. 7406.
(50) Godbout, N.; Salahub, D. R.; Andzelm, J.; Wimmer, E. Optimization of Gaussian-Type Basis Sets for Local Spin Density Functional Calculations. Part I. Boron through Neon, Optimization Technique and Validation. *Can. J. Chem.* **1992**, *70* (2), 560−571.
(51) Pettersson, L. G. M.; Wahlgren, U.; Gropen, O. Effective Core Potential Parameters for First- and Second-row Atoms. *J. Chem. Phys.* **1987**, *86* (4), 2176−2184.
(52) Durbin, T. D.; Lince, J. R.; Didziulis, S. V.; Shuh, D. K.; Yarmoff, J. A. Soft X-ray Photoelectron Spectroscopy Study of the Interaction of Cr with MoS_2(0001). *Surf. Sci.* **1994**, *302* (3), 314−328.
(53) Mullins, D. R.; Lyman, P. F.; Overbury, S. H. Interaction of S with W(001). *Surf. Sci.* **1992**, *277* (1), 64−76.
(54) Nesbitt, H. W.; Berlich, A. G.; Harmer, S. L.; Uhlig, I.; Bancroft, G. M.; Szargan, R. Identification of Pyrite Valence Band Contributions Using Synchrotron-Excited X-ray Photoelectron Spectroscopy. *Am. Mineral.* **2004**, *89* (2−3), 382−389.
(55) von Barth, U.; Grossmann, G. Dynamical Effects in X-ray Spectra and the Final-State Rule. *Phys. Rev. B* **1982**, *25* (8), No. 5150.
(56) Kukk, E.; Bozek, J. D.; Sheehy, J. A.; Langhoff, P. W.; Berrah, N. Angular Distribution of Molecular-Field- and Spin-Orbit-Split Sulfur 2p Photoemission in OCS: A Sensitive Probe of the Molecular Environment. *J. Phys. B:At., Mol. Opt. Phys.* **2000**, *33* (1), No. L51.
(57) Weinhardt, L.; Fuchs, O.; Batchelor, D.; Bär, M.; Blum, M.; Denlinger, J. D.; Yang, W.; Schöll, A.; Reinert, F.; Umbach, E.; Heske, C. Electron-Hole Correlation Effects in Core-Level Spectroscopy Probed by the Resonant Inelastic Soft X-ray Scattering Map of C_{60}. *J. Chem. Phys.* **2011**, *135* (10), No. 104705.
(58) Hennies, F.; Polyutov, S.; Minkov, I.; Pietzsch, A.; Nagasono, M.; Ågren, H.; Triguero, L.; Piancastelli, M.-N.; Wurth, W.; Gel'mukhanov, F.; Föhlisch, A. Dynamic Interpretation of Resonant X-ray Raman Scattering: Ethylene and Benzene. *Phys. Rev. A* **2007**, *76* (3), No. 032505.
(59) Hennies, F.; Pietzsch, A.; Berglund, M.; Föhlisch, A.; Schmitt, Th.; Strocov, V.; Karlsson, H. O.; Andersson, J.; Rubensson, J.-E. Resonant Inelastic Scattering Spectra of Free Molecules with Vibrational Resolution. *Phys. Rev. Lett.* **2010**, *104* (19), No. 193002.
(60) Ertan, E.; Savchenko, V.; Ignatova, N.; da Cruz, V. V.; Couto, R. C.; Eckert, S.; Fondell, M.; Dantz, M.; Kennedy, B.; Schmitt, T.; Pietzsch, A.; Föhlisch, A.; Gel'mukhanov, F.; Odelius, M.; Kimberg, V. Ultrafast Dissociation Features in RIXS Spectra of the Water Molecule. *Phys. Chem. Chem. Phys.* **2018**, *20* (21), 14384−14397.
(61) Gelmukhanov, F.; Ågren, H. X-Ray Resonant Scattering Involving Dissociative States. *Phys. Rev. A* **1996**, *54* (1), No. 379.
(62) Fuchs, O.; Zharnikov, M.; Weinhardt, L.; Blum, M.; Weigand, M.; Zubavichus, Y.; Bär, M.; Maier, F.; Denlinger, J. D.; Heske, C.; Grunze, M.; Umbach, E. Isotope and Temperature Effects in Liquid Water Probed by X-ray Absorption and Resonant X-ray Emission Spectroscopy. *Phys. Rev. Lett.* **2008**, *100* (2), No. 027801.
(63) Weinhardt, L.; Weigand, M.; Fuchs, O.; Bär, M.; Blum, M.; Denlinger, J. D.; Yang, W.; Umbach, E.; Heske, C. Nuclear Dynamics in the Core-Excited State of Aqueous Ammonia Probed by Resonant Inelastic Soft X-ray Scattering. *Phys. Rev. B* **2011**, *84* (10), No. 104202.
(64) Weinhardt, L.; Benkert, A.; Meyer, F.; Blum, M.; Wilks, R. G.; Yang, W.; Bär, M.; Reinert, F.; Heske, C. Nuclear Dynamics and Spectator Effects in Resonant Inelastic Soft X-ray Scattering of Gas-Phase Water Molecules. *J. Chem. Phys.* **2012**, *136* (14), No. 144311.
(65) Weinhardt, L.; Hauschild, D.; Steininger, R.; Wansorra, C.; Yang, W.; Heske, C. Local and Symmetry-Resolved Electronic Structure of Liquid Dimethyl Sulfoxide from Resonant Inelastic Soft X-ray Scattering. *J. Phys. Chem. Lett.* **2024**, *15*, 10576−10582.

https://doi.org/10.1021/photonsci.6c00007
Photon Sci. XXXX, XXX, XXX−XXX